



Review: Friction and Lubrication with High Water Content Crosslinked Hydrogels

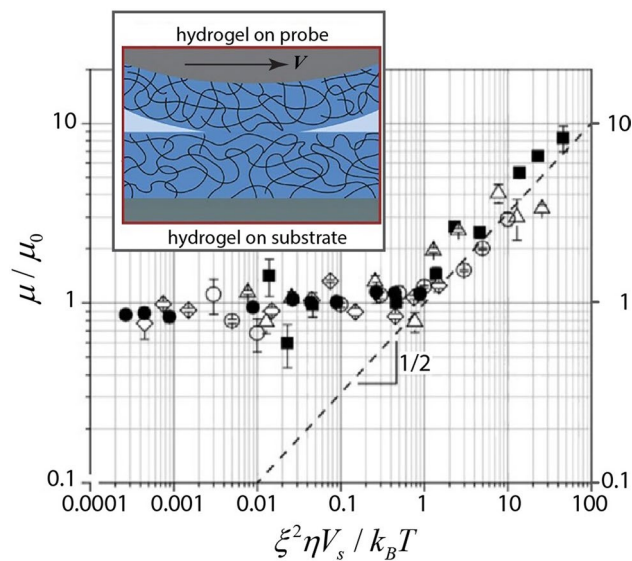
Shabnam Z. Bonyadi¹ · Md. Mahmudul Hasan¹ · Jiho Kim¹ · Samsul Mahmood² · Kyle D. Schulze² · Alison C. Dunn¹

Received: 15 May 2020 / Accepted: 12 October 2020
© Springer Science+Business Media, LLC, part of Springer Nature 2020

Abstract

As soft aqueous hydrogels have moved from new materials to the basis for real engineered devices in the last 20 years, their surface friction and lubrication are emerging as critical aspects of their function. The flexibility to alter and augment their mechanical and surface properties through control of the crosslinked 3D polymer networks has produced materials with diverse surface behaviors, even with the relatively simple composition of a single monomer and crosslink chemistry. Correspondingly with new understandings of the bulk behavior of hydrogels has been the identification of the mechanisms that govern the lubricity and frictional response under dynamic sliding conditions. Here we review these efforts, closely examining and identifying the internal and external influences that drive tribological response in high water content crosslinked hydrogels. The roles of surface structure, elasticity, contact response, charge, water interaction and water flow are addressed here as well as current synthesis and testing methods. We also collect open questions as well as the future needs to fully understand and exploit the surface properties of hydrogels for sliding performance.

Graphical Abstract



Keywords Hydrogels · Aqueous lubrication · Lubrication curve

Shabnam Z. Bonyadi, Md. Mahmudul Hasan, Jiho Kim, and Samsul Mahmood contributed equally to this work.

Extended author information available on the last page of the article

1 Introduction

Tunable soft and aqueous gels, also known as hydrogels, are one of the leading soft matter surrogates for active matter; they are engineered for both temporary and permanent medical prostheses such as catheter coatings, soft contact lenses, and valves [1]. Many of these devices interact directly with dynamic biological interfaces, fully integrated with metabolism, immune response, and other functions, all the while experiencing the mechanical environment of complex sliding speeds, bearing forces, and contact durations. Controlling the motions of slip, that is, the friction and lubrication, is critical to proper function. Crosslinked hydrogels are often thought to be inherently lubricious, but in fact there is a broad spectrum of friction and lubricating abilities.

The lubrication of hydrogels was first described by lubricated sliding of engineering materials in that there are regimes of fluid-controlled lubrication and material-controlled lubrication that loosely resemble hydrodynamic and boundary friction, but the similarities past that are scant. Launched in part by seminal work by JP Gong summarized in a 2006 review of hydrogel lubrication [2], the field of hydrogel friction and lubrication has expanded quickly, with over 200 archival articles published since then under the topic of “hydrogel lubrication” as reported by Web of Science [3]. Efforts over the past ~20 years have sought to identify the ways in which the unique properties of hydrogels control their sliding behavior, which has subsequently required the development of new experimental techniques and data interpretation.

The aim of this review is to present a summary of the most important considerations for hydrogel lubrication, including the mechanics of hydrogel materials, mechanisms of friction and lubrication, updated testing techniques, water-network interactions and flow, and surface structures and designs. A thorough understanding of the origins of hydrogel lubrication and friction will allow for their surfaces to be engineered for applications of the future.

2 Models of Elasticity for Single and Multi-network Hydrogels

For solid materials, mechanical behavior is traditionally defined by the constitutive stress-strain relations expressing stress as a function of strain and strain rate [4]. For many isotropic engineering materials, the response is characterized as initially being linear-elastic: that is stress rising proportionally with strain, up to a limit where after the material either fractures or begins to plastically deform. When deformations and strains are small in the proportional limit the response may be approximated by the three-dimensional tensor

$$\sigma_{ij} = 2GE_{ij} + \lambda\delta_{ij}E_{kk},$$

also known as Hooke’s law. Here, the expression for the stress tensor (σ) is related to the shear modulus (G) of the material, the applied strain (E), the Kronecker delta function (δ), and Lame first parameter (λ) of the material.

Hydrogels, conversely, have high and non-linear strains before failure, which is also typical in hyper-elastic elastomers [5, 6]. In their fully swollen and hydrated form, hydrogels can withstand extremely large compressive and tensile strains with little to no permanent distortion prior to failure [7–9]. Polyacrylamide samples (86% water content), for example, during tensile experiments reached strains up to 1200% before failure [10].

Two unique properties of hydrogels appear to dominate their response to strains: (1) water content governs the elastic response in the linear-elastic regime (typically strains $\ll 40\%$), and (2) crosslink density/network characteristics determine fracture toughness [9]. Several models have been used in an attempt to recapitulate the complex responses observed in these biological and bio-inspired materials and include the Mooney-Rivlin model, the Neo-Hookean Model, and the Ogden model [11–14]. Each model has its limitations, as most were not specifically developed to handle a hydration-dependent, multi-network material. However, experimental and computational validation has found case-specific solutions and applicable strain ranges for hydrogels [15–17].

Contact mechanics measurements, critical to evaluating the tribological performance of a hydrogel, performed in the linear-elastic range suggest that bulk hydrogel response to compressive loads is dependent upon the osmotic pressure of the hydrogel and is consistent with Hertzian predictions over several timescales [18, 19]. Additional measurements showed that this was geometry dependent, suitable for solid (or thick) samples that lack sharp edges [20, 21]. For example, by changing a solid hydrogel indenting probe to a thin-walled design the mechanical response (contact area to force) became nearly linear, and by indenting a hydrogel with a conic punch locally exceeded the osmotic pressure of the gel allowing fluid flow.

While strains are traditionally high at failure for hydrogels [6, 7, 22–24] stresses are typically very low (on the order of kilopascals); this remains one of the major hurdles in more robust applications of hydrogels in medicine [1]. A potential solution is to supplement the original hydrogel with another material that enhances its properties. Multi-network hydrogels containing a brittle, strong component synthesized to increase strength along with a typical softer, weaker hydrogel constituent that maintains other advantageous qualities such as low coefficient of friction, is one of the primary ways to address this concern [25–31]. Another emerging method is to synthesize nanocomposite hydrogels that use physically

confined particles in the gel to modify the overall mechanical properties [32–35]. The strategy is derived from tribological particulate additives to PTFE to reduce wear rates [36]. The goal of both methods is to open the possibilities for new types of soft scaffolding in biological applications and

medicine [28]. The incorporation of these complex hydrogels as tribological testing materials could expand the ranges of stresses and deformations simultaneously measured to achieve diverse biologically relevant test conditions. The composition of multi-network and nanocomposite hydrogels

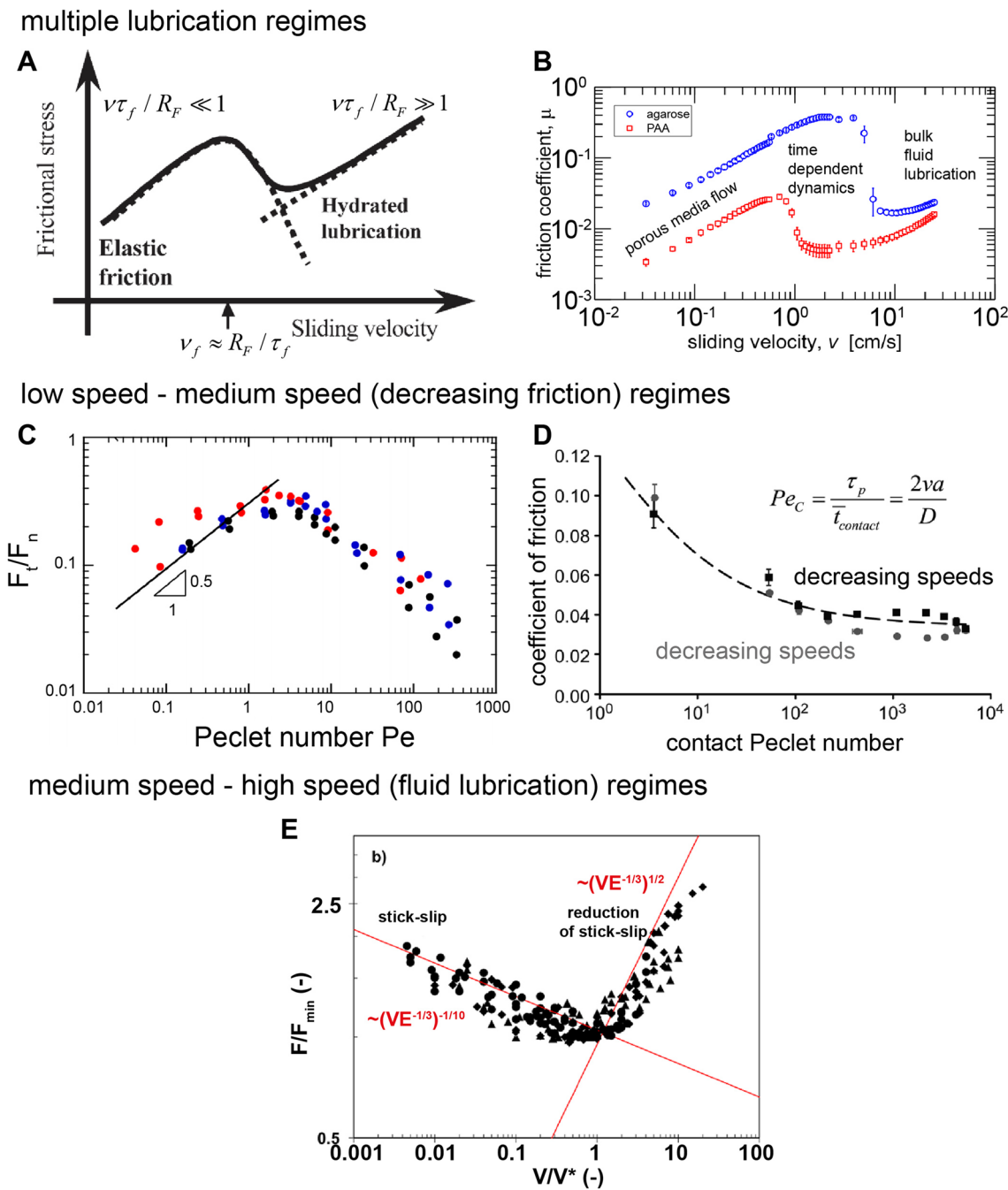


Fig. 1 Lubrication curves for hydrogels. **a–b** Overall shape of the hydrogel lubrication curve. Under increasing sliding speed, friction increases at low speeds, decreases at medium speeds, and increases again at high speeds [2] Reprinted with permission from Royal Society of Chemistry, [42] Printed with permission from Proceedings of the National Academy of Sciences of the United States of America.

c Low-medium speed regimes [41]. Reprinted (adapted) with permission. Copyright (2018) American Chemical Society. **d** Medium speed regime only. Reproduced from Ref. [40] with permission from the Royal Society of Chemistry. **e** Medium–high speed regimes [38]. Reprinted (adapted) with permission. Copyright (2018) American Chemical Society

is rich with variation in mechanical responses and may vary strongly between networks composed of similar materials, but dissimilar in synthesis techniques and concentrations. Because of the possibility of designing hydrogels with such a wide array of mechanical properties, the hyper-elastic models must be validated on a case-by-case basis [8, 33].

3 Mechanisms of Friction and Lubrication

3.1 Hydrogel/Solid Friction

The most common friction measurements and models occur by placing a material of interest against a countersurface which is inert, or lacks the properties of the material of interest. Early pioneering work by Gong et al. placed hydrogels against glass surfaces and established an adsorption-repulsion model of friction based on polymer physics [37]. In the repulsion model, the friction response is modeled as a shear stress under shear driven Couette flow with a gap height due to repulsion between the gel and countersurface. In the adsorption model, surface forces between the hydrogel and countersurface modulate the friction based on time rates of adsorption and desorption, which are determined by the overall nature of the hydrogel as adhesive or repulsive to the countersurface. The two models were tested extensively and found to describe systems tested under moderate pressures. More recent papers by the Espinosa-Marzal group, Dunn group, and Burton group [38–42] expand the two-regime model into multiple regimes along a continuum of conditions such as the driving speed of the sliding component (Fig. 1).

At the microscale, the characteristic sizes of indenters and countersurfaces (hundreds of micrometers to millimeters) far outreach the effective mesh size of the hydrogel (single to tens of nanometers). The microscale forces applied tend to probe the bulk, which determines the mechanical response and surface response more than the surface forces. Thus, the friction regimes are derived from the interaction between the probe, the hydrogel polymer mesh, and the solvent, either within the hydrogel or entrained at the interface. At slow driving speeds, the relatively long duration effects of pressure-driven solvent exudation or creep occur, and have two possible effects: increasing contact area and local dehydration. At the opposite extreme of fast sliding speeds, the hydrogel surface acts more as a compliant surface in which the solvent has no time to flow out of the hydrogel, and other effect like viscoelasticity can dominate the response [39].

While friction and lubrication of hydrogels can be revealed against a stiff, impermeable countersurface, the interface is at the extreme of asymmetry with respect to these properties. Glass, sapphire, or other hard probes have historically been the standard for inert probes, as they are less prone to tribo-chemical reactions with ductile metals or composites. However, that assumption is not as reliable when considering the polymeric components of the hydrogel with the elements that make up glass, specifically silicon and oxygen. Thus, while it is most convenient to use traditional setups with hard probes to make measurements and inferences regarding hydrogel friction and lubrication, the results are limited to specific hydrogels which are truly chemically inert.

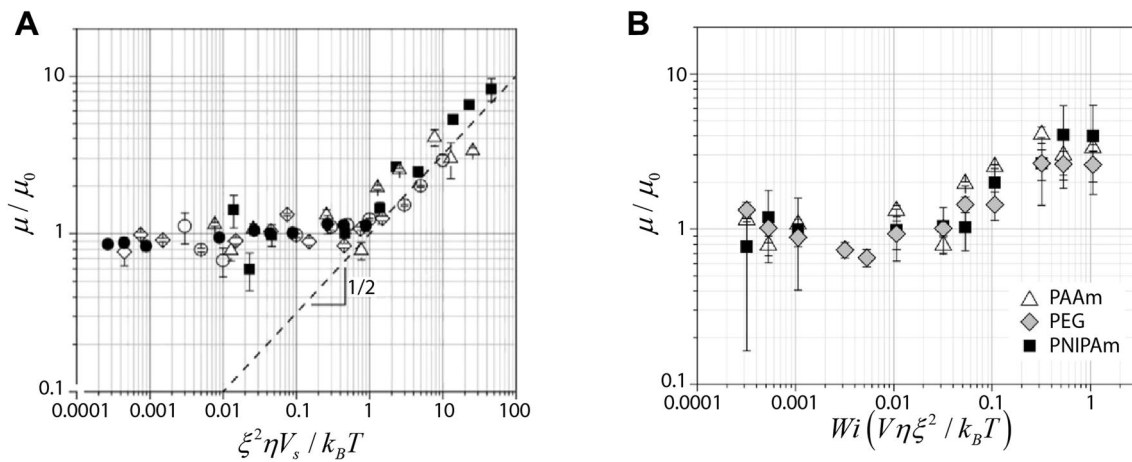


Fig. 2 **a** A speed-independent friction regime at moderate sliding speeds is shown by the normalized friction coefficient plotted versus Weissenberg number, which is a function of the sliding speed. [46]

Reproduced with permission from Springer. **b** Medium–high speed regimes. The friction is constant at medium speeds in this study [48]. Reproduced with permission from Elsevier

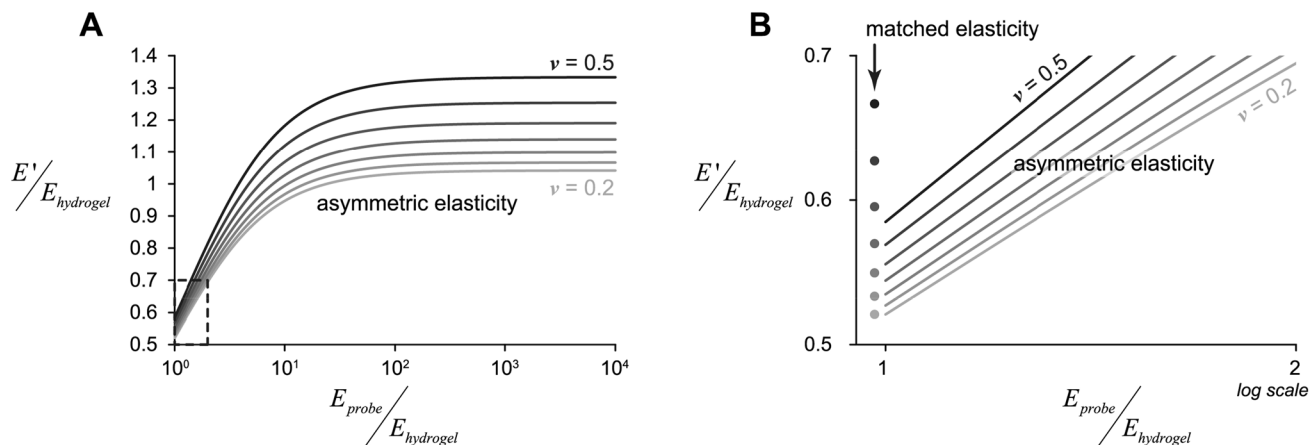


Fig. 3 **a** The effective Hertz contact stiffness E' is the inverse combination of the moduli of the surfaces in contact. For strongly asymmetric elasticity shown on the x-axis, E' is a positive multiplier of the hydrogel modulus (y-axis). The multiplier is higher as the hydrogel approaches incompressibility. The Poisson ratio of the probe is taken

to be a constant at $\nu = 0.25$. **b** For matched elasticity and Poisson ratio in Gemini contact, the multiplier is always < 1 . The discontinuity in the multipliers for an elasticity ratio of 1 is due to the assumption of $\nu_{\text{PROBE}} = 0.25$ with varying ν_{HYDROGEL} ; in Gemini contact they are equivalent at the values shown

3.2 Hydrogel Self-mated 'Gemini' Friction

Hydrogels are quickly becoming model systems to understand biological lubrication due to the similarity between their composition and that of tissues such as cartilage, ocular and digestive epithelia [43]. However, the friction and lubrication of those systems occur between surfaces which are *both* soft and hydrated: cartilage sliding on cartilage, for example. Experiments achieving this setup require significant changes to existing instrumentation, as well as new ways of synthesizing the probe to be a soft material. Rheometers have been modified to include a hydrogel disk adhered to both top and bottom plates, allowing for the center to slip in rotation [44]. Also, significant work has been done to fabricate soft hemispherical probes, constant-pressure probes, and spheres as probes [20, 42]. Removing the stiff, impermeable surface from the interface can allow more direct probing of the inherent lubricating abilities of hydrogels because there is no obvious direct contact with a dissimilar counter-surface. In fact, hydrophilic hydrogels sliding in soft–soft contact have been described by multiple theories, including polymer relaxation lubrication [45], mesh-size lubrication [46], and charge [44]. The measurements associated with these theories have identified a speed-independent regime at sliding speeds slow enough to avoid viscous drag penalties (Fig. 2) [41, 47, 48].

What has been more clearly observed is that soft–soft contacts in probe-based tribology measurements easily remain at very low contact pressures because contact areas grow readily under load due to the compliance. As a demonstration, consider a contact with asymmetric elasticity, i.e. a hard probe against a soft hydrogel. The effective Hertz contact modulus E' is a positive multiplier of the elastic modulus

of the hydrogel for asymmetries $E_{\text{PROBE}}/E_{\text{HYDROGEL}} = 10$ or above, and a negative multiplier if the asymmetry is less; the exact conversion ratio depends upon the Poisson ratio of the hydrogel (Fig. 3a). For Gemini interfaces with matched elasticity and Poisson ratio, the ratio of effective modulus to hydrogel modulus is a maximum of 0.67 and a minimum of 0.52; it cannot be greater than 1 (Fig. 3b). Thus, the effective contact stiffness for Gemini contacts remains low, and in turn reduces the maximum pressure of the interface, as Hertz contact predicts $p_0 \propto (E')^{1/3}$.

This low pressure is associated with low friction coefficients [43] and more fundamental hypotheses regarding the nature of the contact between two hydrogel surfaces are needed. For example, it remains unclear whether a hydrophilic polymer mesh with stable water shells surrounding the polymer chains can directly ‘contact’ other similar polymer chains in a slip interface [49, 50]. Even so, the composition of the hydrogel determines its effective mesh size ξ , which is a predictive parameter for the stiffness, permeability, and energy dissipation [51]. This composition presents at the surface, and a more dilute composition results in much lower friction in this configuration [46]. Further work in which the polymer chain interaction is more controlled is expected to expand these theories.

3.3 Scale-Dependent Friction

According to scaling law, the contribution of different factors associated with friction varies in different length scales [52]. Thus, the frictional behavior of hydrogels found at the macroscale may not be similar at the nanoscale. Because most biological contact occurs at the nanoscale, researchers find immense interest to understand the frictional behavior of hydrogels at the nanoscale [53, 54]. The friction of hard

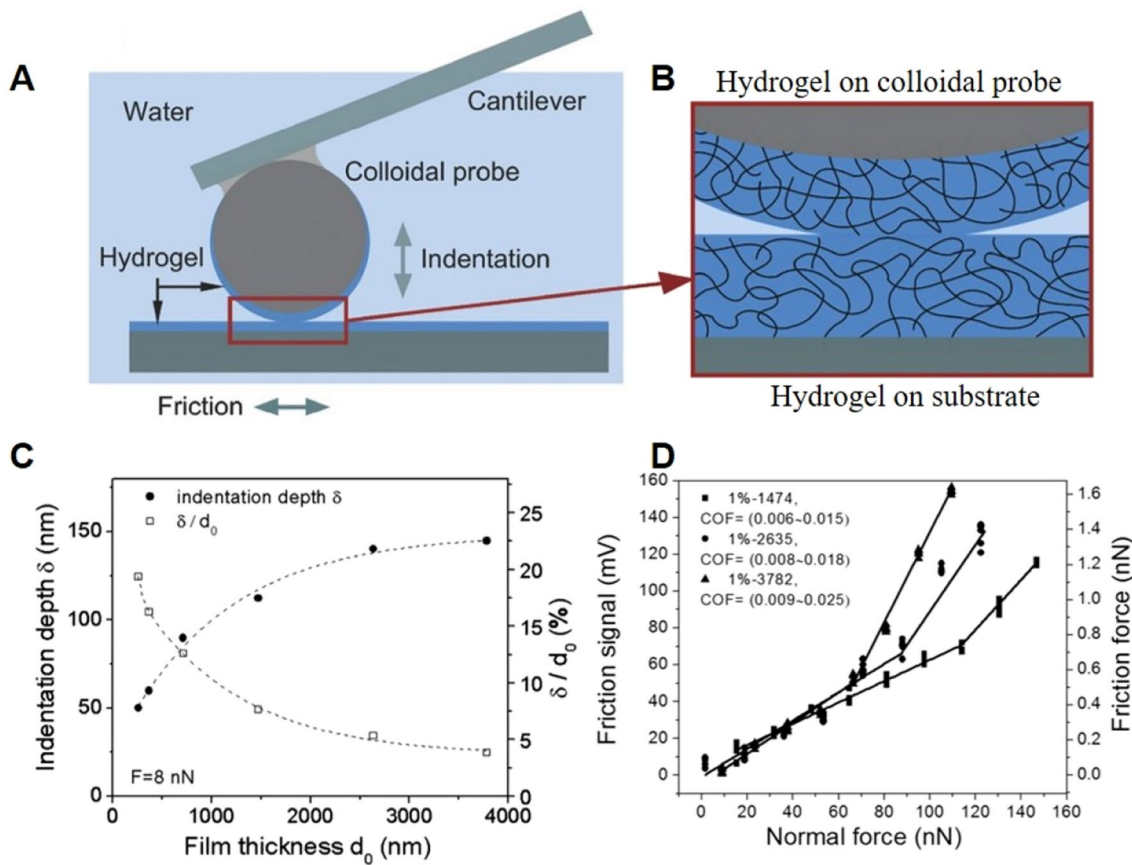


Fig. 4 **a, b** A schematic depiction of the indentation and friction experiments of surface-attached hydrogel using an AFM. **c** Indentation depth is a function of film thickness for constant loading (load: 8 nN). Thinner film behaves stiffer, and less compressible compared to the thicker film. **d** Friction tests (velocity = 20 μms^{-1} and sliding distance = 10 μm) of the thicker hydrogel samples (PDMAA-co-MABP) in water. Here, 1%—1474, 1%—2635, and 1%—3782

samples have 1% MABP and film thicknesses in water are 1474 nm, 2635 nm, and 3782 nm, respectively. At low normal load, COFs are similar irrespective of gel thickness due to small compression region compared to film thickness. In contrast, COF is increasing with film thickness at high normal load due to the stronger deswelling factor. Reproduced with permission from the WILEY-VCH Verlag GmbH [67]

probe-hydrogel contact at the nanoscale largely depends on the geometry of the contact, adhesive contact interaction, contact deformation, and ambient conditions [55]. High surface roughness on the hard probe increases the real contact area with soft hydrogels [56]. Also, it increases the nano adhesion due to the long-range non-contact capillary forces [57]. Apart from adhesion due to surface roughness, adhesion, itself (one type of surface force) becomes always significant in proportion to the volume force (e.g., body force) at smaller scale. Using DMT theory, this small-scale adhesion can be described properly [58]. Different intrinsic properties of the polymer, such as glass transition temperature [59], and activation energy for molecular motion [60] are different on the surface compared to the bulk, which also dominate the frictional behavior. In addition, different experimental parameters, such as, speed [61], load [62], sliding distance [63], temperature [64], pH [64, 65], and

prestressed conditions [66] are reported as critical factors in nanoscale hydrogel friction.

The Gemini contact (hydrogel-hydrogel contact) of the surface-attached hydrogel (Fig. 4a, b) at nanoscale (thickness can be as low as 260 nm) largely depends on the load, loading rate, polymer to crosslink density, and the local solvent deswelling dynamics through the porous polymer network [67]. In a static compression test, thinner layers have higher local relaxation zone compared to the total layer thickness and thus, the surface behaves stiffer (Fig. 4c). This layer thickness effect depends on the load. When Gemini contact slides against each-other at a high normal load, the solvent deswells more strongly for thicker samples, and hence, the coefficient of friction (COF) increases with thickness (Fig. 4d).

3.4 Fast- and Slow-Sliding Speeds Regimes

At fast sliding speeds, the relationship between the sliding speed and the resulting friction tends toward a power relationship regardless of the testing method. This occurs for hydrogels both in a self-mated configuration and against a stiff impermeable countersurface (see Fig. 1a, b, e). This is generally understood to be due to full-film lubrication, or hydrodynamic lubrication, in which the surfaces are completely separated by the pressurized fluid film. As the sliding speed continues to increase, viscous drag of the fluid film increases, and increases friction slightly. While many groups report a hydrodynamic-like regime at high slip speeds [42, 68, 69], the ability to pressurize a film between porous surfaces is counteracted by the possibility of pressure-driven flow through the pores. Multiple groups now use dimensionless parameters like the Péclet number to show how competitive effects can describe transitions in friction [40, 41]. However, if one considers the internal restriction to flow away from contact due to the small effective mesh size on the order of 1 s to 10 s of nanometers, a pressure in the water film between the hydrogel surface and countersurface could be maintained. Further studies describe how the elastic or viscoelastic character of the hydrogels interacts with the fluid film generation, which is known as elastohydrodynamic lubrication (EHL) [39, 70].

While much work agrees that high-speed sliding is primarily controlled by the properties of the fluid film, the contrasting slow-velocity regime is influenced by a number of environmental and material variables. Specifically, the fundamental materials interactions in addition to time-dependent changes under loading are considered to be most important. In the case of repulsive hydrogels, the friction is often the lowest at the slowest speeds tested or considered [48, 70, 71]. If pressures are high enough, the dwell time causes pressure-driven flow, or local drainage [18, 40, 41, 72], which increases both contact area and friction. Some groups are also beginning to consider this fluid drainage during sliding from the near-surface region in a ‘hydrodynamic’ sense, in which the fluid motion controls the deformation, and thus the friction response [42, 73–75]. Finally, the combination of speed-dependent effects and surface adhesions has been considered in detail at the nanoscale [47].

4 Water-Network Interactions and Flow

When compressed under constant loads, hydrogels have demonstrated a time-dependent relaxation response similar to creep [21, 72, 76, 77]. Due to the liquid–solid duality of hydrogels, this phenomenon has historically been described as “poroelastic” or driven by the ability of the fluid

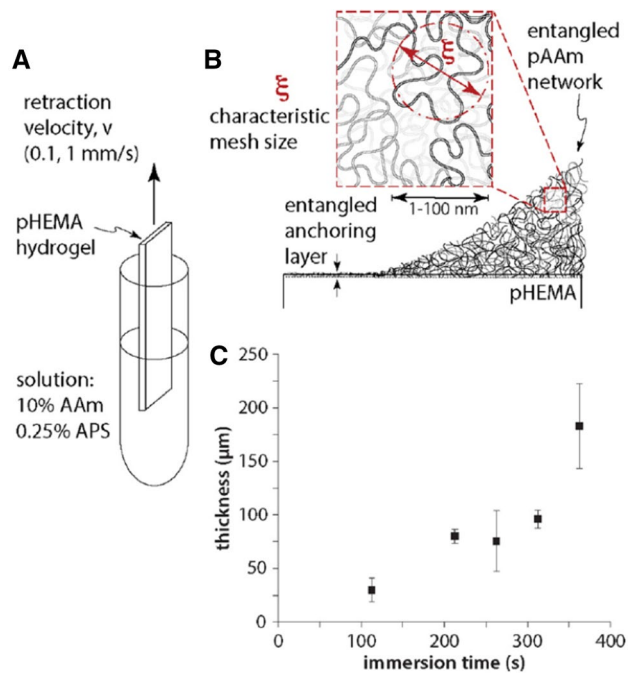


Fig. 5 Retracting a flat substrate during chemical polymerization without crosslinking produced a thick, lubricious layer of polyacrylamide atop a substrate of less-lubricious polyHEMA. Reproduced with permission from ASME [27]

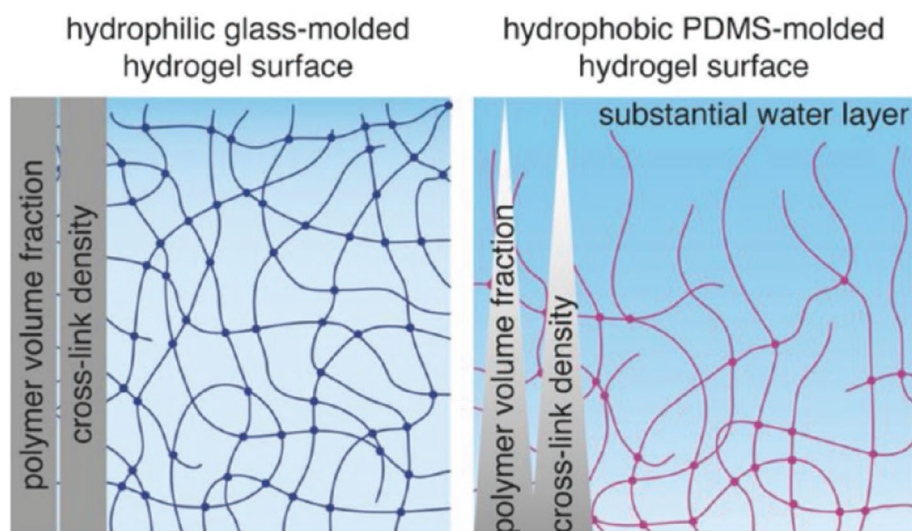
component to drain through the pores of the solid component of the hydrogel. In this model, the pore-size is the mesh-size of the hydrogel which is on the order of nanometers [46, 78] rather than the micrometer and millimeter pore-size of traditional porous materials such as sponges or cartilage. Suo et al. thoroughly demonstrates the responses to many indenter shapes and forces, and attributes the response to this model [21, 72, 76]. However, as water has a size on the order of 3 angstroms, the smaller, thermally-active channel size is a significant hindrance to the flow rate through the bulk of the gel. It has been demonstrated for the water to pass through hydrogel bulk the osmotic pressure of the hydrogel must be exceeded by the pressing pressure [18, 19]. For typical contact profiles under compression these pressures are not achievable under contact but are achievable with sharp shapes such as conics or knives edges near the tip. For cases where flow is not possible, the time-dependent relaxation may be related to the thermal reorganization of the hydrogel.

5 Surface Structures and Designs

5.1 Lubricious Surface Layers by Design

Lubricity of hydrogels has been correlated with water content [42, 46]. However, when the polymer concentration

Fig. 6 (Left) Based on mechanical testing and in situ spectroscopy, multiple groups find that a glass mold for chemically-crosslinked hydrogels imparts a “neat” surface with uniform composition in the near-surface region. (Right) Contrasting to that is a layer depleted of crosslinks and polymer concentration imparted to the hydrogel surface by a hydrophobic mold. Reproduced with permission from WILEY-VCH Verlag GmbH [86]



and/or crosslink concentration is very low, the character of the hydrogel may deviate from an elastic solid, and not have sufficient structure to hold together as a solid material. Thus, lubricity has a practical limit of bulk fragility. A system which leverages the higher- and lower-water content hydrogels is a laminate structure with a compliant lubricious hydrogel presenting at the surface and a tougher hydrogel as its substrate. This exists both in commercial soft contact lenses [79] and in the laboratory [80, 81]. An exceedingly lubricious, and even slimy surface, can be fabricated by growing an entangled layer of polymer from a crosslinked hydrogel substrate [27] (Fig. 5). While promising, optimizing this system for broad design of laminate composites is not yet in the open literature.

5.2 Mold Materials and Imparted Properties

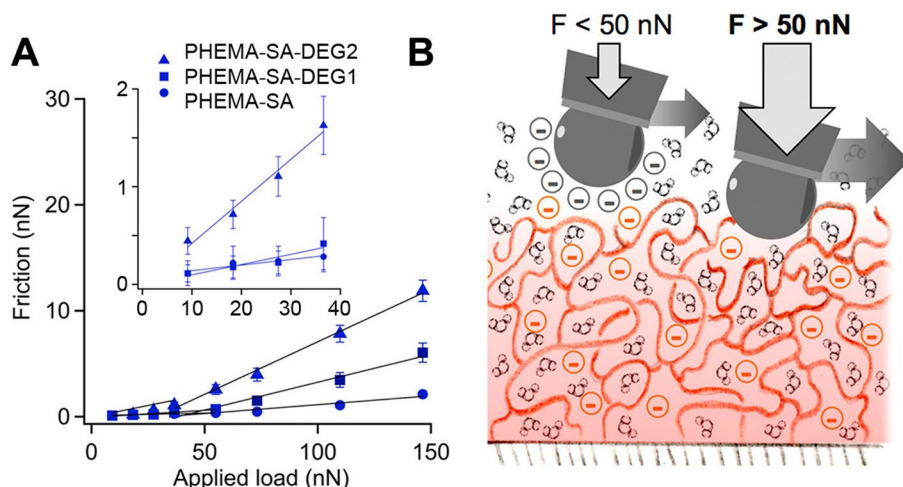
Hydrogels that are simultaneously crosslinked and polymerized like polyacrylamide [82, 83] have often been molded against borosilicate laboratory glassware to act as a mechanical boundary. It was assumed that the mold just determined the geometry of the hydrogel surface without affecting the local chemistry of the synthesized surface. This assumption has recently been scrutinized due to the variety of mold materials available, as well as an early discovery of a less-dense surface layer [84]. For a single chemistry of polyacrylamide prepared in an identical protocol with the exception of the mold material on a spectrum between hydrophilic glass and hydrophobic bulk polymers, a softer surface extending down micrometers was discovered to be associated with the more hydrophobic molds [85, 86]. The softer surface was hypothesized to be sparse at its outer extent and increase in density toward the bulk, where the “bulk” being some effective screening distance from the mold (Fig. 6). In the same line as

the early discovery, recent work demonstrates a swollen outer layer on polyacrylamide that can be worn away, but re-emerges over time [87]. Authors hypothesized that a swollen surface region will always emerge due to the way that the solvated chains reconfigure to maximize the exclusion of water shells. Thus, there is ample opportunity to leverage mold materials and novel synthesis methods to engineer the surfaces of hydrogels to have a surface composition that enhances lubricity.

5.3 Charged Hydrogel or Charged Solvent Effects on Lubrication

The charge of the hydrogel influences its interactions with the solvent and countersurface, and thus, its frictional response. Previous work has shown charged hydrogel surfaces with equal sign can trap fluid at the interface, and the ions of the fluid separate based on their charge. The ion rearrangement at the interface creates a bilayer domain of hydrated ions that requires higher loads to maintain the density, and thus the integrity of the hydrated layer [49]. The trapped fluid at the interface experiences an osmotic pressure due to the load applied and remains at the interface during sliding [88]. Therefore, the friction at the interface can be expressed using the Navier-Stokes equations for shear stresses produced due to fluid flow. Because the fluid flow dictates the measured friction, the quality and contents of the solvent strongly influence the lubrication regime of the interface. Adding charged surfactants to the solution can further decrease friction of the gel-mated interfaces by remaining at the interface and strengthening the repulsion of the two surfaces [89]. Furthermore, charged ions in the solution can be trapped at the interface, creating sub-nanometer hydration shells [50]. The development of a hydration layer due to charge repulsion at the hydrogel interface gives rise to

Fig. 7 Low COF was observed due to electrostatic repulsion between the two negatively charged mating faces (silica probe and the deprotonated carboxylic acid functions at the polymer surface). In contrast, at high load (> 50 nN), the probe started to deform the brush films, and consequently, the friction increased [65]. Reprinted (adapted) with permission from [65]. Copyright (2017) American Chemical Society



superlubricity, or very low friction values. Superlubricity has also been achieved at the interface of a hydrogel copolymer of two zwitterionic polymers and a sapphire probe when water was used as the lubricant [90]. The strength of adsorption of water molecules onto the surface of the charged hydrogel was great enough to maintain a fluid layer between the hydrogel and the hard probe at a range of speeds and loads (Fig. 7) [65]. Therefore, the charge of the hydrogel has a strong influence on its frictional behavior.

6 Updated Testing Techniques

Hydrogels tribological performance, i.e. their coefficients of friction and wear rates against surfaces and their mechanical response to contact remain exceptionally pertinent in identifying their use as engineering materials [1, 32]. The ability to directly observe the interactions of soft material interfaces and determine contact deformation using *in situ* microscopy

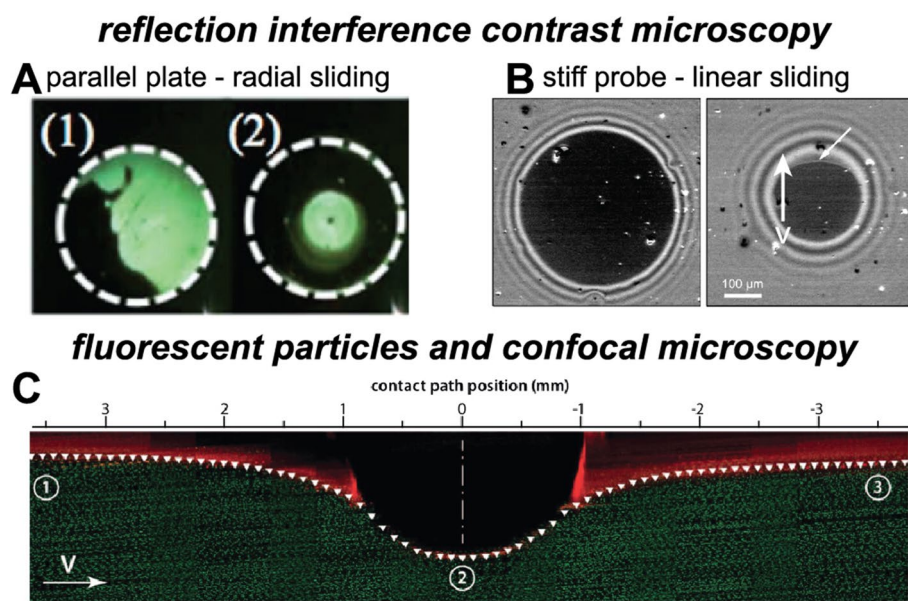


Fig. 8 Methods of viewing hydrogel contact. **a** Heterogeneous contact of a hydrogel against a glass plate during radial sliding due to low compressive pressures allowing water to be trapped at the interface [113]. Increasing sliding speed from image 1 to 2 led to dramatic decrease in the contact area. **b** A hydrogel film sliding laterally underneath a fixed glass lens. In static contact, the contact area is circular (left). Upon sliding (right), contact asymmetry occurs due to loss of contact at the trailing edge, and continued circular shape at the

leading edge. Reprinted (adapted) with permission from [41]. Copyright (2018) American Chemical Society. **c** Composite image of vertically stacked confocal images of a glass probe (black area) applying a load to a rotating hydrogel disk (green fluorescent microspheres) that is submerged in water (red fluorescent microspheres). The white triangles mark the surface profile [39]. Reproduced with permission from Elsevier

[91] was a watershed event as it has allowed direct characterization of mechanical surface properties [92–95], validated non-in situ tribological measurement techniques [53, 55, 96–100], and aided in the development of test devices using soft materials [101–105]. Nanoscale measurements using AFM and bulk measurements using rheology remain effective ways to ascertain physical properties of hydrogels at their respective scales [106–112]. The desire to bridge these properties observed at the nanoscale and macroscale has led to unique testing techniques for hydrogels at the microscale and the mesoscale. The characterization of hydrogels mechanical and tribological performance, as well as the use of hydrogels tribological apparatus for other soft and active matter have advanced with the ability to precisely make measurements at these scales.

Direct optical light measurements at hydrogel surfaces are often confounded by the index of refraction mismatch between the hydrogel and the water it is submerged into prevent de-swelling. A number of methods have been developed to differentiate the refractive index between the swollen gel film and the water such as using a trapezoidal glass prism [113] or crossed polarizers and quarter-wave plates [41]. The images developed by using these methods are shown in Fig. 8a, b. In addition, several techniques have been developed to directly observe these “invisible” surfaces with established methods such as light microscopy and confocal microscopy. Particle exclusion microscopy (PEM) uses either fluorescent or dye particles to act as the primary signal within either the hydrogel itself or within the fluid surrounding the interface; where these particles are absent, the hydrogel must occupy [114]. By mounting a pin-on-disk micro-tribometer in the direct light path of an inverted microscope, PEM has been used to assess the contact mechanics of hydrogels as both probe and counter surface from the indirect observation of the contact area in both static indentation and dynamic sliding [115–119]. Similarly, direct measurements of contact area may also be accomplished with a micro-tribometer and fluorescence confocal microscope by three-dimensional reconstruction of the indented surfaces and probes by adding a small amount of dispersed nano-sized fluorescent particles to the hydrogel samples before polymerization [18, 20, 118]. The indentation is centered along the scanning laser path and a series of images are taken sequentially scanning monotonically at different z heights to develop the surface contour. Inspired by these direct observations, constant-pressure hydrogel probes were designed and generated using a 3D printer to apply controlled pressures to delicate systems such as cell monolayers. The indications of contact in vitro correlated to the coefficient of friction and physical factors that cause cells to signal inflammation, premature cell death, and potentially disease propagation [20, 120–124].

Wear of hydrogel measurements has remained elusive as they easily accommodate compressive forces with large contact areas and rearrangements, begin to de-swell quickly when exposed to air making surface profile measurements with devices such as a scanning white light interferometer difficult, and may inherently have low wear rates against many typical smooth counter-surfaces used in tribology. Efforts to measure a wear rate were successful by reciprocating a highly-rough 3.75 mm radius cylinder ($R_a \sim 8 \mu\text{m}$) against hydrogel surface using a custom micro-tribometer for 30 km varying both speed (1 mm/s and 3 mm/s) and normal load (1–20 mN). The experiments produced large wear scars visible to the naked eye and wear rates (0.1–0.4 mm^3/Nm) as measured by a 3D laser scanning confocal microscope. Additional tensile measurement and analysis with the high wear rates suggest that wear in the gels is a competition between ductile and brittle fracture [125]. Further studies and new testing techniques need to be employed to determine wear rates of hydrogels against smoother bodies and corroborate the high-wear results.

As stated previously, in vitro studies of cell monolayers measured frictional shear stresses with a soft spherical shell hydrogel probe [122, 123]. The studies were performed with a reciprocating micro-tribometer capable of applying micro newton normal loads, measuring Pascal-level stresses, while traveling millimeters of distance (and therefore across many cells) and arranged to run with a simultaneous control sample. The ability to use the spherical hydrogel probe mitigated vertical alignment issues that would cause a stiffer probe to plow through the cells monolayer during the long travel path (~ 1000 cell widths). Other investigators are currently performing friction measurements of hydrogels and cells in vitro with an apparatus similar to a miniaturized rheometer [126, 127]. Here a biological sample (such as resected cornea) is placed against a hydrogel disk of similar size which may be actuated axially and rotationally. The actuator the gel is attached to is equipped with axial load and torque sensors. The torque and axial load collected during the experiment are used to determine the friction coefficients.

7 Closure and Future Perspectives

The behavior of hydrogel materials and surfaces in sliding contacts fundamentally alters prior understandings of lubrication due to their compliance, synthesis methods and surface character, and compliant water-dependent structure that drives transport of the lubricating fluid. The composition of the hydrogel is influential in all of these, especially the monomer concentration(s) and monomer/crosslinker ratio [82, 83, 128, 129]. Further, surface layers

or composite regions can enhance the lubricity without losing other desirable properties of the bulk such as stiffness.

With medical advances and the increasing prevalence of human-machine interfaces, hydrogels are lead contenders for mediating a wide variety of biological-synthetic interfaces. As they become the basis for engineered structures and devices on a large scale, other engineering properties such as ductility, fatigue, and fracture toughness are beginning to be investigated [24, 130, 131]. Adding the lubrication and surface performance as an aspect of their overall design will ensure reliable and robust operation of hydrogel-based devices for existing and future applications.

Acknowledgements The authors are grateful for all researchers in this field and their contributions. SZB, ACD, MMH, and JK were supported by the National Science Foundation awards 1563087 and 1751945. KDS and SM were supported by Auburn University Samuel Ginn College of Engineering. Professor Nicholas D. Spencer is the inspiration for this updated review.

Author's Contribution ACD and KDS outlined this work, wrote, and edited. SZB, MMH, JK, and SM wrote, prepared figures, and edited.

Funding Authors SZB, ACD, MMH, and JK acknowledge support from the National Science Foundation (NSF) awards numbers 1563087 and 1751945. KDS and SM were supported by Auburn University Samuel Ginn College of Engineering.

Data Availability The authors do not have original experimental data in this review. Thus this declaration is not applicable.

Compliance with Ethical Standards

Conflict of interest The authors declare that they have no conflicts of interest and no competing interests in writing this review.

References

1. Kirschner, C.M., Anseth, K.S.: Hydrogels in healthcare: from static to dynamic material microenvironments. *Acta Mater.* **61**, 931–944 (2013). <https://doi.org/10.1016/j.actamat.2012.10.037>
2. Gong, J.P.: Friction and lubrication of hydrogels—its richness and complexity. *Soft Matter* **2**, 544 (2006). <https://doi.org/10.1039/b603209p>
3. Analytics, C.: Web of Science Citation Report for topic words “Hydrogel lubrication.” (2020)
4. Sadd, M.H.: *Elasticity: Theory, Applications, and Numerics*. Elsevier, Amsterdam (2009)
5. Rosendahl, P.L., Drass, M., Felger, J., Schneider, J., Becker, W.: Equivalent strain failure criterion for multiaxially loaded incompressible hyperelastic elastomers. *Int. J. Solids Struct.* **166**, 32–46 (2019). <https://doi.org/10.1016/j.ijsolstr.2019.01.030>
6. Naficy, S., Brown, H.R., Razal, J.M., Spinks, G.M., Whitten, P.G.: Progress toward robust polymer hydrogels. *Aust. J. Chem.* **64**, 1007 (2011). <https://doi.org/10.1071/CH11156>
7. Huang, T., Xu, H., Jiao, K., Zhu, L., Brown, H.R., Wang, H.: A novel hydrogel with high mechanical strength: a macromolecular microsphere composite hydrogel. *Adv. Mater.* **19**, 1622–1626 (2007). <https://doi.org/10.1002/adma.200602533>
8. Gong, J.P., Katsuyama, Y., Kurokawa, T., Osada, Y.: Double-network hydrogels with extremely high mechanical strength. *Adv. Mater.* **15**, 1155–1158 (2003). <https://doi.org/10.1002/adma.200304907>
9. Nakayama, A., Kakugo, A., Gong, J.P., Osada, Y., Takai, M., Erita, T., Kawano, S.: High mechanical strength double-network hydrogel with bacterial cellulose. *Adv. Funct. Mater.* **14**, 1124–1128 (2004). <https://doi.org/10.1002/adfm.200305197>
10. Yang, C., Yin, T., Suo, Z.: Polyacrylamide hydrogels. I. Network imperfection. *J. Mech. Phys. Solids* **131**, 43–55 (2019). <https://doi.org/10.1016/j.jmps.2019.06.018>
11. Mihai, L.A., Goriely, A.: How to characterize a nonlinear elastic material? A review on nonlinear constitutive parameters in isotropic finite elasticity. In: *Proceedings of the Royal Society A: Mathematical, Physical and Engineering Sciences*. Royal Society Publishing (2017)
12. Kim, B., Lee, S.B., Lee, J., Cho, S., Park, H., Yeom, S., Park, S.H.: A comparison among Neo-Hookean model, Mooney-Rivlin model, and Ogden model for Chloroprene rubber. *Int. J. Precis. Eng. Manuf.* **13**, 759–764 (2012). <https://doi.org/10.1007/s12541-012-0099-y>
13. Rivlin, R.S.: Large elastic deformations of isotropic materials VI. Further developments of the general theory. *Philos. Trans. R. Soc. Lond. Ser. A* **241**, 379–397 (1948). <https://doi.org/10.1098/rsta.1948.0024>
14. Ogden, R.W.: Large deformation isotropic elasticity—on the correlation of theory and experiment for incompressible rubberlike solids. *Proc. R. Soc. Lond. A. Math. Phys. Sci.* **326**, 565–584 (1972). <https://doi.org/10.1098/rspa.1972.0026>
15. Faghihi, S., Karimi, A., Jamadi, M., Imani, R., Salarian, R.: Graphene oxide/poly(acrylic acid)/gelatin nanocomposite hydrogel: experimental and numerical validation of hyperelastic model. *Mater. Sci. Eng. C* **38**, 299–305 (2014). <https://doi.org/10.1016/j.msec.2014.02.015>
16. Sasson, A., Patchornik, S., Eliasy, R., Robinson, D., Haj-Ali, R.: Hyperelastic mechanical behavior of chitosan hydrogels for nucleus pulposus replacement—experimental testing and constitutive modeling. *J. Mech. Behav. Biomed. Mater.* **8**, 143–153 (2012). <https://doi.org/10.1016/j.jmbbm.2011.12.008>
17. Van Der Sman, R.G.M.: Hyperelastic models for hydration of cellular tissue. *Soft Matter* **11**, 7579–7591 (2015). <https://doi.org/10.1039/c5sm01032b>
18. Schulze, K.D., Hart, S.M., Marshall, S.L., O'Bryan, C.S., Urueña, J.M., Pitenis, A.A., Sawyer, W.G., Angelini, T.E.: Polymer osmotic pressure in hydrogel contact mechanics. *Biotribology* (2017). <https://doi.org/10.1016/j.biotri.2017.03.004>
19. Bhattacharyya, A., O'Bryan, C., Ni, Y., Morley, C.D., Taylor, C.R., Angelini, T.E.: Hydrogel compression and polymer osmotic pressure. *Biotribology* **22**, 100125 (2020). <https://doi.org/10.1016/j.biotri.2020.100125>
20. Marshall, S.L., Schulze, K.D., Hart, S.M., Urueña, J.M., McGhee, E.O., Bennett, A.I., Pitenis, A.A., O'Bryan, C.S., Angelini, T.E., Sawyer, W.G.: Spherically capped membrane probes for low contact pressure tribology. *Biotribology* **11**, 69–72 (2017). <https://doi.org/10.1016/j.biotri.2017.03.008>
21. Hu, Y., Zhao, X., Vlassak, J.J., Suo, Z.: Using indentation to characterize the poroelasticity of gels. *Appl. Phys. Lett.* **96**, 121904 (2010). <https://doi.org/10.1063/1.3370354>
22. Stammen, J.A., Williams, S., Ku, D.N., Guldberg, R.E.: Mechanical properties of a novel PVA hydrogel in shear and unconfined compression. *Biomaterials* **22**, 799–806 (2001). [https://doi.org/10.1016/S0142-9612\(00\)00242-8](https://doi.org/10.1016/S0142-9612(00)00242-8)

23. Li, J., Liu, H., Wang, C., Huang, G.: A facile method to fabricate hybrid hydrogels with mechanical toughness using a novel multifunctional cross-linker. *RSC Adv.* **7**, 35311–35319 (2017). <https://doi.org/10.1039/C7RA05645A>

24. Bai, R., Yang, Q., Tang, J., Morelle, X.P., Vlassak, J., Suo, Z.: Fatigue fracture of tough hydrogels. *Extrem. Mech. Lett.* **15**, 91–96 (2017). <https://doi.org/10.1016/j.eml.2017.07.002>

25. Rudy, A., Kuliasha, C., Uruena, J., Rex, J., Schulze, K.D., Stewart, D., Angelini, T., Sawyer, W.G., Perry, S.S.: Lubricous hydrogel surface coatings on polydimethylsiloxane (PDMS). *Tribol. Lett.* (2017). <https://doi.org/10.1007/s11249-016-0783-7>

26. Lin, P., Ma, S., Wang, X., Zhou, F.: Molecularly engineered dual-crosslinked hydrogel with ultrahigh mechanical strength, toughness, and good self-recovery. *Adv. Mater.* **27**, 2054–2059 (2015). <https://doi.org/10.1002/adma.201405022>

27. Pitenis, A.A., Uruena, J.M., Nixon, R.M., Bhattacharjee, T., Krick, B.A., Dunn, A.C., Angelini, T.E., Sawyer, W.G.: Lubricity from polymer entangled networks on hydrogels. *J. Tribol.* **138**, 042102 (2016)

28. Li, C., Rowland, M.J., Shao, Y., Cao, T., Chen, C., Jia, H., Zhou, X., Yang, Z., Scherman, O.A., Liu, D.: Responsive double network hydrogels of interpenetrating DNA and CB[8] host-guest supramolecular systems. *Adv. Mater.* **27**, 3298–3304 (2015). <https://doi.org/10.1002/adma.201501102>

29. Chen, Q., Zhu, L., Zhao, C., Wang, Q., Zheng, J.: A robust, one-pot synthesis of highly mechanical and recoverable double network hydrogels using thermoreversible sol-gel polysaccharide. *Adv. Mater.* **25**, 4171–4176 (2013). <https://doi.org/10.1002/adma.201300817>

30. Gong, Z., Zhang, G., Zeng, X., Li, J., Li, G., Huang, W., Sun, R., Wong, C.: High-strength, tough, fatigue resistant, and self-healing hydrogel based on dual physically cross-linked network. *ACS Appl. Mater. Interfaces.* **8**, 24030–24037 (2016). <https://doi.org/10.1021/acsami.6b05627>

31. Gong, J.P.: Materials both tough and soft. *Science* **344**, 161–162 (2014)

32. Gaharwar, A.K., Peppas, N.A., Khademhosseini, A.: Nanocomposite hydrogels for biomedical applications. *Biotechnol. Bioeng.* **111**, 441–453 (2014). <https://doi.org/10.1002/bit.25160>

33. Liu, J., Chen, C., He, C., Zhao, J., Yang, X., Wang, H.: synthesis of graphene peroxide and its application in fabricating super extensible and highly resilient nanocomposite hydrogels. *ACS Nano* (2012). <https://doi.org/10.1021/nn302874v>

34. Pasqui, D., Atrei, A., Giani, G., De Cagna, M., Barbucci, R.: Metal oxide nanoparticles as cross-linkers in polymeric hybrid hydrogels. *Mater. Lett.* **65**, 392–395 (2011). <https://doi.org/10.1016/j.matlet.2010.10.053>

35. Peppas, N.A., Hilt, J.Z., Khademhosseini, A., Langer, R.: Hydrogels in biology and medicine: from molecular principles to biomanotechnology. *Adv. Mater.* **18**, 1345 (2006)

36. Sawyer, W.G., Freudenberg, K.D., Bhimaraj, P., Schadler, L.S.: A study on the friction and wear behavior of PTFE filled with alumina nanoparticles. *Wear* **254**, 573–580 (2003). [https://doi.org/10.1016/S0043-1648\(03\)00252-7](https://doi.org/10.1016/S0043-1648(03)00252-7)

37. Gong, J., Osada, Y.: Gel friction: a model based on surface repulsion and adsorption. *J. Chem. Phys.* **109**, 8062–8068 (1998). <https://doi.org/10.1063/1.477453>

38. Shoaib, T., Heintz, J., Lopez-Berganza, J.A., Muro-Barrios, R., Egner, S.A., Espinosa-Marzal, R.M.: Stick-slip friction reveals hydrogel lubrication mechanisms. *Langmuir* **34**, 756–765 (2018). <https://doi.org/10.1021/acs.langmuir.7b02834>

39. McGhee, E.O., Pitenis, A.A., Urueña, J.M., Schulze, K.D., McGhee, A.J., O'Bryan, C.S., Bhattacharjee, T., Angelini, T.E., Sawyer, W.G.: In situ measurements of contact dynamics in speed-dependent hydrogel friction. *Biotribology* **13**, 23–29 (2018). <https://doi.org/10.1016/j.biotri.2017.12.002>

40. Reale, E.R., Dunn, A.C.: Poroelasticity-driven lubrication in hydrogel interfaces. *Soft Matter* **13**, 428–435 (2017). <https://doi.org/10.1039/c6sm02111e>

41. Delavoipière, J., Tran, Y., Verneuil, E., Heurtefu, B., Hui, C.Y., Chateauminois, A.: Friction of poroelastic contacts with thin hydrogel films. *Langmuir* **34**, 9617–9626 (2018). <https://doi.org/10.1021/acs.langmuir.8b01466>

42. Cuccia, N.L., Pothineni, S., Wu, B., Méndez Harper, J., Burton, J.C.: Pore-size dependence and slow relaxation of hydrogel friction on smooth surfaces. *Proc. Natl. Acad. Sci.* **117**, 11247–11256 (2020). <https://doi.org/10.1073/pnas.1922364117>

43. Dunn, A.C., Sawyer, W.G., Angelini, T.E.: Gemini interfaces in aqueous lubrication with hydrogels. *Tribol. Lett.* **54**, 59–66 (2014). <https://doi.org/10.1007/s11249-014-0308-1>

44. Gong, J.P., Kagata, G., Osada, Y.: Friction of gels 4 friction on charged gels. *J. Phys. Chem. B* **103**, 6007–6014 (1999). <https://doi.org/10.1021/jp990256v>

45. Pitenis, A.A., Urueña, J.M., Schulze, K.D., Nixon, R.M., Dunn, A.C., Krick, B.A., Sawyer, W.G., Angelini, T.E.: Polymer fluctuation lubrication in hydrogel gemini interfaces. *Soft Matter* **10**, 8955–8962 (2014). <https://doi.org/10.1039/c4sm01728e>

46. Urueña, J.M., Pitenis, A.A., Nixon, R.M., Schulze, K.D., Angelini, T.E., Gregory Sawyer, W.: Mesh size control of polymer fluctuation lubrication in gemini hydrogels. *Biotribology* **1–2**, 24–29 (2015). <https://doi.org/10.1016/j.biotri.2015.03.001>

47. Shoaib, T., Espinosa-Marzal, R.M.: Insight into the viscous and adhesive contributions to hydrogel friction. *Tribol. Lett.* **66**, 1–14 (2018). <https://doi.org/10.1007/s11249-018-1045-7>

48. Pitenis, A.A., Sawyer, W.G.: Lubricity of high water content aqueous gels. *Tribol. Lett.* **66**, 1–7 (2018). <https://doi.org/10.1007/s11249-018-1063-5>

49. Gaisinskaya, A., Ma, L., Silbert, G., Sorkin, R., Tairy, O., Goldberg, R., Kampf, N., Klein, J.: Hydration lubrication: exploring a new paradigm. *Faraday Discuss.* **156**, 217 (2012). <https://doi.org/10.1039/c2fd00127f>

50. Ma, L., Gaisinskaya-kipnis, A., Kampf, N., Klein, J.: Origins of hydration lubrication. *Nat. Commun.* **6**, 1–6 (2015). <https://doi.org/10.1038/ncomms7060>

51. Zhang, J., Peppas, N.A.: Synthesis and characterization of pH- and temperature-sensitive poly(methacrylic acid)/poly(N-isopropylacrylamide) interpenetrating polymeric networks. *Macromolecules* **33**, 102–107 (2000). <https://doi.org/10.1021/ma991398q>

52. Tambe, N.S., Bhushan, B.: Scale dependence of micro/nano-friction and adhesion of MEMS/NEMS materials, coatings and lubricants. *Nanotechnology* **15**, 1561–1570 (2004). <https://doi.org/10.1088/0957-4484/15/11/033>

53. Li, H., Choi, Y.S., Rutland, M.W., Atkin, R.: Nanotribology of hydrogels with similar stiffness but different polymer and crosslinker concentrations. *J. Colloid Interface Sci.* **563**, 347–353 (2020). <https://doi.org/10.1016/j.jcis.2019.12.045>

54. You, S., Li, J., Zhu, W., Yu, C., Mei, D., Chen, S.: Nanoscale 3D printing of hydrogels for cellular tissue engineering. *J. Mater. Chem. B* **6**, 2187–2197 (2018). <https://doi.org/10.1039/c8tb00301g>

55. Liamas, E., Connell, S.D., Ramakrishna, S.N., Sarkar, A.: Probing the frictional properties of soft materials at the nanoscale. *Nanoscale* **12**, 2292–2308 (2020)

56. Mulakaluri, N., Persson, B.N.J.: Adhesion between elastic solids with randomly rough surfaces: Comparison of analytical theory with molecular-dynamics simulations. *EPL* (2011). <https://doi.org/10.1209/0295-5075/96/66003>

57. Pandyala, P., Kim, H.N., Grewal, H.S., Cho, I.J., Yoon, E.S.: Effect of capillary forces on the correlation between nanoscale adhesion and friction of polymer patterned surfaces. *Tribol. Int.* **114**, 436–444 (2017). <https://doi.org/10.1016/j.tribolint.2017.04.045>

58. Ciavarella, M., Joe, J., Papangelo, A., Barber, J.R.: The role of adhesion in contact mechanics. *J. R. Soc. Interface.* (2019). <https://doi.org/10.1098/rsif.2018.0738>

59. Kajiyama, T., Tanaka, K., Takahara, A.: Analysis of surface mobility in polystyrene films with monodisperse and bimodal molecular weights by lateral force microscopy. *Polym. Sci.* **42**, 639–647 (2003)

60. Fu, J., Li, B., Han, Y.: Molecular motions of different scales at thin polystyrene film surface by lateral force microscopy. *J. Chem. Phys.* (2005). <https://doi.org/10.1063/1.1961228>

61. Tambe, N.S., Bhushan, B.: Micro/nanotribological characterization of PDMS and PMMA used for BioMEMS/NEMS applications. *Ultramicroscopy* (2005). <https://doi.org/10.1016/J.ULTRAMIC.2005.06.050>

62. Bogdanovic, G., Tiberg, F., Rutland, M.W.: Sliding friction between cellulose and silica surfaces. *Langmuir* **17**, 5911–5916 (2001). <https://doi.org/10.1021/la010330c>

63. Ramakrishna, S.N., Cirelli, M., Divandari, M., Benetti, E.M.: Effects of lateral deformation by thermoresponsive polymer brushes on the measured friction forces. *Langmuir* **33**, 4164–4171 (2017). <https://doi.org/10.1021/acs.langmuir.7b00217>

64. Nordgren, N., Rutland, M.W.: Tunable nanolubrication between dual-responsive polyionic grafts. *Nano Lett.* **9**, 2984–2990 (2009). <https://doi.org/10.1021/nl901411e>

65. Dehghani, E.S., Ramakrishna, S.N., Spencer, N.D., Benetti, E.M.: Controlled crosslinking is a tool to precisely modulate the nanomechanical and nanotribological properties of polymer brushes. *Macromolecules* **50**, 2932–2941 (2017). <https://doi.org/10.1021/acs.macromol.6b02409>

66. Solares, S.D.: Nanoscale effects in the characterization of viscoelastic materials with atomic force microscopy: coupling of a quasi-three-dimensional standard linear solid model with in-plane surface interactions. *Beilstein J. Nanotechnol.* **7**, 554–571 (2016). <https://doi.org/10.3762/bjnano.7.49>

67. Li, K., Pandiyarajan, C.K., Prucker, O., Rühe, J.: On the lubrication mechanism of surfaces covered with surface-attached hydrogels. *Macromol. Chem. Phys.* **217**, 526–536 (2016). <https://doi.org/10.1002/macp.201500243>

68. Kurokawa, T., Tominaga, T., Katsuyama, Y., Kuwabara, R., Furukawa, H., Osada, Y., Gong, J.P.: Elastic-hydrodynamic transition of gel friction. *Langmuir* **21**, 8643–8648 (2005). <https://doi.org/10.1021/la050635h>

69. Kim, J., Dunn, A.C.: Soft hydrated sliding interfaces as complex fluids. *Soft Matter* **12**, 6536–6546 (2016). <https://doi.org/10.1039/C6SM00623J>

70. Kagata, G., Gong, P., Osada, Y.: Friction of gels. 6. Effects of sliding velocity and viscoelastic responses of the network. *J. Phys. Chem. B.* **106**, 4596–4601 (2002). <https://doi.org/10.1021/jp012380w>

71. Kim, J., Dunn, A.C.: Thixotropic mechanics in soft hydrated sliding interfaces. *Tribol. Lett.* (2018). <https://doi.org/10.1007/s11249-018-1056-4>

72. Chan, E.P., Hu, Y., Johnson, P.M., Suo, Z., Stafford, C.M.: Spherical indentation testing of poroelastic relaxations in thin hydrogel layers. *Soft Matter* **8**, 1492 (2012). <https://doi.org/10.1039/c1sm06514a>

73. McGhee, E.O., Urueña, J.M., Pitenis, A.A., Sawyer, W.G.: Temperature-dependent friction of gemini hydrogels. *Tribol. Lett.* **67**, 1–7 (2019). <https://doi.org/10.1007/s11249-019-1229-9>

74. Murakami, T., Yarimitsu, S., Nakashima, K., Sakai, N., Yamaguchi, T., Sawae, Y., Suzuki, A.: Biphasic and boundary lubrication mechanisms in artificial hydrogel cartilage: a review. *Proc. Inst. Mech. Eng. Part H J. Eng. Med.* **229**, 864–878 (2015). <https://doi.org/10.1177/0954411915611160>

75. Murakami, T., Sakai, N., Yamaguchi, T., Yarimitsu, S., Nakashima, K., Sawae, Y., Suzuki, A.: Evaluation of a superior lubrication mechanism with biphasic hydrogels for artificial cartilage. *Tribol. Int.* **89**, 19–26 (2015). <https://doi.org/10.1016/j.triboint.2014.12.013>

76. Hu, Y., Suo, Z.: Viscoelasticity and poroelasticity in elastomeric gels. *Acta Mech. Solida Sin.* **25**, 441–458 (2012). [https://doi.org/10.1016/S0894-9166\(12\)60039-1](https://doi.org/10.1016/S0894-9166(12)60039-1)

77. Blum, M.M., Ovaert, T.C.: Experimental and numerical tribological studies of a boundary lubricant functionalized porous viscoelastic PVA hydrogel in normal contact and sliding. *J. Mech. Behav. Biomed. Mater.* **14**, 248–258 (2012). <https://doi.org/10.1016/j.jmbbm.2012.06.009>

78. Oyen, M.L.: Mechanical characterisation of hydrogel materials. *Int. Mater. Rev.* **59**, 44–59 (2014). <https://doi.org/10.1179/1743280413Y.0000000022>

79. Dunn, A.C., Urueña, J.M., Huo, Y., Perry, S.S., Angelini, T.E., Sawyer, W.G.: Lubricity of surface hydrogel layers. *Tribol. Lett.* **49**, 371–378 (2013). <https://doi.org/10.1007/s11249-012-0076-8>

80. Simmons, C.S., Ribeiro, A.J.S., Pruitt, B.L.: Formation of composite polyacrylamide and silicone substrates for independent control of stiffness and strain. *Lab Chip* **13**, 646–649 (2013). <https://doi.org/10.1039/c2lc41110e>

81. Yu, Y., Yuk, H., Parada, G.A., Wu, Y., Liu, X., Nabzdyk, C.S., Youcef-Toumi, K., Zang, J., Zhao, X.: Multifunctional “hydrogel skins” on diverse polymers with arbitrary shapes. *Adv. Mater.* (2019). <https://doi.org/10.1002/adma.201807101>

82. Yeung, T., Georges, P.C., Flanagan, L.A., Marg, B., Ortiz, M., Funaki, M., Zahir, N., Ming, W., Weaver, V., Janmey, P.A.: Effects of substrate stiffness on cell morphology, cytoskeletal structure, and adhesion. *Cell Motil. Cytoskeleton* **60**, 24–34 (2005). <https://doi.org/10.1002/cm.20041>

83. Denisin, A.K., Pruitt, B.L.: Tuning the range of polyacrylamide gel stiffness for mechanobiology applications. *ACS Appl. Mater. Interfaces* **8**, 21893–21902 (2016). <https://doi.org/10.1021/acsami.5b09344>

84. Sudre, G., Hourdet, D., Cousin, F., Creton, C., Tran, Y.: Structure of surfaces and interfaces of poly(N, N-dimethylacrylamide) hydrogels. *Langmuir* **28**, 12282–12287 (2012). <https://doi.org/10.1021/la301417x>

85. Meier, Y.A., Zhang, K., Spencer, N.D., Simič, R.: Linking friction and surface properties of hydrogels molded against materials of different surface energies. *Langmuir* **35**, 15805–15812 (2019). <https://doi.org/10.1021/acs.langmuir.9b01636>

86. Gombert, Y., Simič, R., Roncoroni, F., Dübner, M., Geue, T., Spencer, N.D.: Structuring hydrogel surfaces for tribology. *Adv. Mater. Interfaces* (2019). <https://doi.org/10.1002/admi.201901320>

87. Bonyadi, S.Z., Atten, M., Dunn, A.C.: Self-regenerating compliance and lubrication of polyacrylamide hydrogels. *Soft Matter* **15**, 8728–8740 (2019). <https://doi.org/10.1039/c9sm01607d>

88. Persson, B.N.J., Scaraggi, M.: Some Comments on Hydrogel and Cartilage Contact Mechanics and Friction. *Tribol. Lett.* **66**, 1–6 (2018). <https://doi.org/10.1007/s11249-017-0973-y>

89. Kamada, K., Furukawa, H., Kurokawa, T., Tada, T., Tominaga, T., Nakano, Y., Gong, J.P.: Surfactant-induced friction reduction for hydrogels in the boundary lubrication regime. *J. Phys. Condens. Matter.* (2011). <https://doi.org/10.1088/0953-8984/23/28/284107>

90. Wang, Z., Li, J., Liu, Y., Luo, J.: Macroscale superlubricity achieved between zwitterionic copolymer hydrogel and sapphire in water. *Mater. Des.* **188**, 108441 (2020). <https://doi.org/10.1016/j.matdes.2019.108441>

91. Chaudhury, M.K., Whitesides, G.M.: Direct measurement of interfacial interactions between semispherical lenses and flat sheets of poly(dimethylsiloxane) and their chemical derivatives. *Langmuir* **7**, 1013–1025 (1991). <https://doi.org/10.1021/la00053a033>

92. Shull, K.R.: Contact mechanics and the adhesion of soft solids, (2002)

93. Lorenz, B., Krick, B.A., Mulakaluri, N., Smolyakova, M., Dieluweit, S., Sawyer, W.G., Persson, B.N.J.: Adhesion: role of bulk viscoelasticity and surface roughness. *J. Phys. Condens. Matter* **25**, 225004 (2013). <https://doi.org/10.1088/0953-8984/25/22/225004>

94. Greenwood, J.A., Johnson, K.L.: Oscillatory loading of a viscoelastic adhesive contact. *J. Colloid Interface Sci.* **296**, 284–291 (2006). <https://doi.org/10.1016/j.jcis.2005.08.069>

95. Shull, K.R., Ahn, D., Chen, W., Flanigan, C.M., Crosby, A.J.: Axisymmetric adhesion tests of soft materials. *Macromol. Chem. Phys.* **199**, 489–511 (1998). [https://doi.org/10.1002/\(SICI\)1521-3935\(19980401\)199:4%3c489:AID-MACP489%3e3.0.CO;2-A](https://doi.org/10.1002/(SICI)1521-3935(19980401)199:4%3c489:AID-MACP489%3e3.0.CO;2-A)

96. Aulin, C., Shchukarev, A., Lindqvist, J., Malmström, E., Wågberg, L., Lindström, T.: Wetting kinetics of oil mixtures on fluorinated model cellulose surfaces. *J. Colloid Interface Sci.* **317**, 556–567 (2008). <https://doi.org/10.1016/j.jcis.2007.09.096>

97. Wahl, K.J., Asif, S.A.S., Greenwood, J.A., Johnson, K.L.: Oscillating adhesive contacts between micron-scale tips and compliant polymers. *J. Colloid Interface Sci.* **296**, 178–188 (2006). <https://doi.org/10.1016/j.jcis.2005.08.028>

98. Bhushan, B., Israelachvili, J.N., Landman, U.: Nanotribology: Friction, wear and lubrication at the atomic scale. *Nature* (1995). <https://doi.org/10.1038/374607a0>

99. Roba, M., Duncan, E.G., Hill, G.A., Spencer, N.D., Tosatti, S.G.P.: Friction measurements on contact lenses in their operating environment. *Tribol. Lett.* **44**, 387–397 (2011). <https://doi.org/10.1007/s11249-011-9856-9>

100. Serner, O., Aeschlimann, R., Zürcher, S., Scales, C., Riederer, D., Spencer, N.D., Tosatti, S.G.P.: Tribological classification of contact lenses: from coefficient of friction to sliding work. *Tribol. Lett.* **63**, 1–13 (2016). <https://doi.org/10.1007/s11249-016-0696-5>

101. McDonald, J.C., Whitesides, G.M.: Poly(dimethylsiloxane) as a material for fabricating microfluidic devices. *Acc. Chem. Res.* **35**, 491–499 (2002). <https://doi.org/10.1021/ar010110q>

102. Abate, A.R., Lee, D., Do, T., Holtze, C., Weitz, D.A.: Glass coating for PDMS microfluidic channels by sol-gel methods. *Lab Chip* **8**, 516–518 (2008). <https://doi.org/10.1039/b800001h>

103. Rim, Y.S., Bae, S.-H., Chen, H., De Marco, N., Yang, Y.: Recent progress in materials and devices toward printable and flexible sensors. *Adv. Mater.* **28**, 4415–4440 (2016). <https://doi.org/10.1002/adma.201505118>

104. Crosby, A.J., Hageman, M., Duncan, A.: Controlling polymer adhesion with “pancakes”. *Langmuir* **21**, 11738–11743 (2005). <https://doi.org/10.1021/la051721k>

105. Shepherd, R.F., Stokes, A.A., Nunes, R.M.D., Whitesides, G.M.: Soft machines that are resistant to puncture and that self seal. *Adv. Mater.* **25**, 6709–6713 (2013). <https://doi.org/10.1002/adma.201303175>

106. Nalam, P.C., Gosvami, N.N., Caporizzo, M.A., Composto, R.J., Carpick, R.W.: Nano-rheology of hydrogels using direct drive force modulation atomic force microscopy. *Soft Matter* **11**, 8165–8178 (2015). <https://doi.org/10.1039/c5sm01143d>

107. Nalam, P.C., Lee, H.S., Bhatt, N., Carpick, R.W., Eckmann, D.M., Composto, R.J.: Nanomechanics of pH-responsive, drug-loaded, bilayered polymer grafts. *ACS Appl. Mater. Interfaces* **9**, 12936–12948 (2017). <https://doi.org/10.1021/acsami.6b14116>

108. Li, A., Benetti, E.M., Tranchida, D., Clasohm, J.N., Schönherr, H., Spencer, N.D.: Surface-grafted, covalently cross-linked hydrogel brushes with tunable interfacial and bulk properties. *Macromolecules* **44**, 5344–5351 (2011). <https://doi.org/10.1021/ma2006443>

109. Bhamla, M.S., Chai, C., Rabiah, N.I., Frostad, J.M., Fuller, G.G.: Instability and breakup of model tear films. *Investig. Ophthalmol. Vis. Sci.* **57**, 949–958 (2016). <https://doi.org/10.1167/iovs.15-18064>

110. Bhamla, M.S., Balemans, C., Fuller, G.G.: Dewetting and deposition of thin films with insoluble surfactants from curved silicone hydrogel substrates. *J. Colloid Interface Sci.* **449**, 428–435 (2015). <https://doi.org/10.1016/j.jcis.2015.01.002>

111. Kandow, C.E., Georges, P.C., Janmey, P.A., Beningo, K.A.: Polyacrylamide hydrogels for cell mechanics: steps toward optimization and alternative uses. *Methods Cell Biol.* **83**, 29–46 (2007)

112. Wen, Q., Basu, A., Janmey, P.A., Yodh, A.G.: Non-affine deformations in polymer hydrogels. *Soft Matter* **8**, 8039–8049 (2012)

113. Yamamoto, T., Kurokawa, T., Ahmed, J., Kamita, G., Yashima, S., Furukawa, Y., Ota, Y., Furukawa, H., Gong, J.P.: In situ observation of a hydrogel-glass interface during sliding friction. *Soft Matter* **10**, 5589–5596 (2014). <https://doi.org/10.1039/c4sm00338a>

114. Schulze, K.D., Bennett, A.I., Marshall, S.L., Rowe, K.G., Dunn, A.C.: Real area of contact in a soft transparent interface by particle exclusion microscopy. *ASME J. Tribol.* **138**, 041404 (2016)

115. Pham, J.T., Schellenberger, F., Kappl, M., Butt, H.J.: From elasticity to capillarity in soft materials indentation. *Phys. Rev. Mater.* **1**, 015602 (2017). <https://doi.org/10.1103/PhysRevMaterials.1.015602>

116. Graham, B.T., Moore, A.C., Burris, D.L., Price, C.: Sliding enhances fluid and solute transport into buried articular cartilage contacts. *Osteoarthr. Cartil.* **25**, 2100–2107 (2017). <https://doi.org/10.1016/j.joca.2017.08.014>

117. McGhee, E.O., Pitenis, A.A., Urueña, J.M., Schulze, K.D., McGhee, A.J., O'Bryan, C.S., Bhattacharjee, T., Angelini, T.E., Sawyer, W.G.: In situ measurements of contact dynamics in speed-dependent hydrogel friction. *Biotribology* **13**, 23–29 (2017). <https://doi.org/10.1016/j.biotri.2017.12.002>

118. Lee, D., Rahman, M.M., Zhou, Y., Ryu, S.: Three-dimensional confocal microscopy indentation method for hydrogel elasticity measurement. *Langmuir* **31**, 9684–9693 (2015). <https://doi.org/10.1021/acs.langmuir.5b01267>

119. Bonyadi, S.Z., Atten, M., Dunn, A.C.: Self-regenerating compliance and lubrication of polyacrylamide hydrogels. *Soft Matter* (2019). <https://doi.org/10.1039/c9sm01607d>

120. Urueña, J.M., Hart, S.M., Hood, D.L., McGhee, E.O., Niemi, S.R., Schulze, K.D., Levings, P.P., Sawyer, W.G., Pitenis, A.A.: Considerations for biotribometers: cells, gels, and tissues. *Tribol. Lett.* **66**, 1–7 (2018). <https://doi.org/10.1007/s11249-018-1094-y>

121. Pitenis, A.A., Urueña, J.M., McGhee, E.O., Hart, S.M., Reale, E.R., Kim, J., Schulze, K.D., Marshall, S.L., Bennett, A.I., Niemi, S.R., Angelini, T.E., Sawyer, W.G., Dunn, A.C.: Challenges and opportunities in soft tribology. *Tribol. Mater. Surfaces Interfaces* **11**, 180–186 (2017). <https://doi.org/10.1080/17515831.2017.1400779>

122. Pitenis, A.A., Urueña, J.M., Hart, S.M., O'Bryan, C.S., Marshall, S.L., Levings, P.P., Angelini, T.E., Sawyer, W.G.: Friction-induced inflammation. *Tribol. Lett.* **66**, 1–13 (2018). <https://doi.org/10.1007/s11249-018-1029-7>

123. Hart, S.M., Degen, G.D., Urueña, J.M., Levings, P.P., Sawyer, W.G., Pitenis, A.A.: Friction-induced apoptosis. *Tribol. Lett.* **67**, 1–12 (2019). <https://doi.org/10.1007/s11249-019-1197-0>

124. McGhee, E.O., Hart, S.M., Urueña, J.M., Sawyer, W.G.: Hydration control of gel-adhesion and muco-adhesion. *Langmuir* **35**, 15769–15775 (2019). <https://doi.org/10.1021/acs.langmuir.9b02816>

125. Bonyadi, S.Z., Dunn, A.C.: Brittle or ductile? Abrasive wear of polyacrylamide hydrogels reveals load-dependent wear mechanisms. *Tribol. Lett.* **68**, 1–14 (2020). <https://doi.org/10.1007/s11249-019-1259-3>

126. Morrison, S., Sullivan, D.A., Sullivan, B.D., Sheardown, H., Schmidt, T.A.: Dose-dependent and synergistic effects of proteoglycan 4 on boundary lubrication at a human cornea-polydimethylsiloxane. *Biointerface Eye Contact Lens Sci. Clin. Pract.* **38**, 27–35 (2012). <https://doi.org/10.1097/ICL.0b013e31823f7041>

127. Korogiannaki, M., Samsom, M., Schmidt, T.A., Sheardown, H.: Surface-functionalized model contact lenses with a bioinspired proteoglycan 4 (PRG4)-grafted layer. *ACS Appl. Mater. Interface* **10**, 30125–30136 (2018). <https://doi.org/10.1021/acsami.8b09755>

128. Urueña, J.M., Pitenis, A.A., Nixon, R.M., Schulze, K.D., Angelini, T.E., Gregory Sawyer, W.: Mesh size control of polymer fluctuation lubrication in gemini hydrogels. *Biotribology* **1–2**, 24–29 (2014). <https://doi.org/10.1016/j.biotri.2015.03.001>

129. Zhang, J., Daubert, C.R., Foegeding, E.A.: Characterization of polyacrylamide gels as an elastic model for food gels. *Rheol. Acta* **44**, 622–630 (2005). <https://doi.org/10.1007/s00397-005-0444-5>

130. Tanaka, Y., Kuwabara, R., Na, Y.H., Kurokawa, T., Gong, J.P., Osada, Y.: Determination of fracture energy of high strength double network hydrogels. *J. Phys. Chem. B* **109**, 11559–11562 (2005). <https://doi.org/10.1021/jp0500790>

131. Kundu, S., Crosby, A.J.: Cavitation and fracture behavior of polyacrylamide hydrogels. *Soft Matter* **5**, 3963–3968 (2009). <https://doi.org/10.1039/b909237d>

Publisher's Note Springer Nature remains neutral with regard to jurisdictional claims in published maps and institutional affiliations.

Affiliations

Shabnam Z. Bonyadi¹ · Md. Mahmudul Hasan¹  · Jiho Kim¹ · Samsul Mahmood²  · Kyle D. Schulze²  · Alison C. Dunn¹ 

✉ Alison C. Dunn
acd@illinois.edu

¹ Department of Mechanical Science & Engineering, Grainger College of Engineering, University of Illinois at Urbana-Champaign, Urbana, IL, USA

² Department of Mechanical Engineering, Samuel Ginn College of Engineering, Auburn University, Auburn, AL, USA